



Signal-to-noise-ratio (SNR) of X-ray imaging scintillators determined by luminescence measurements

D. Cavouras^{a,*}, I. Kandarakis^a, M. Kanellopoulos^a, C.D. Nomicos^b,
G.S. Panayiotakis^c

^aDepartment of Medical Instrumentation Technology, Technological Educational Institution of Athens, Ag. Spyridonos Street, Aigaleo 122 10, Athens, Greece

^bDepartment of Electronics, Technological Educational Institution of Athens, Ag. Spyridonos Street, Aigaleo 122 10, Athens, Greece

^cDepartment of Medical Physics, Medical School, University of Patras, 265 00 Patras, Greece

Abstract

A new method for studying the signal-to-noise-ratio (SNR) of X-ray imaging scintillators was developed. SNR was expressed in terms of the X-ray luminescence efficiency (XLE) the X-ray to emitted light conversion efficiency and the mean light photon energy. Laboratory prepared $\text{Gd}_2\text{O}_2\text{S:Tb}$, $\text{La}_2\text{O}_2\text{S:Tb}$ and $\text{Y}_2\text{O}_2\text{S:Tb}$ scintillator screens were tested and best results were obtained for the 80 mg/cm^2 $\text{Gd}_2\text{O}_2\text{S:Tb}$ screen. The method proposed allows for scintillator comparison on the basis of XLE and wavelength measurements. © 1999 Elsevier Science Ltd. All rights reserved.

1. Introduction

Scintillators in the form of X-ray screens are used in a vast variety of conventional or digital medical imaging applications. A scintillator's role is to detect the incident X-ray beam containing the primary diagnostic information and to convert it into a visible optical signal. The useful information appearing in the resulting image may be quantitatively assessed in terms of the signal-to-noise-ratio (SNR) (Motz and Danos, 1978, Dick and Motz, 1981). The latter is governed by the X-ray detection properties of the scintillator and its ability to produce and efficiently emit optical quanta. A significant amount of primary information conveyed by the input X-ray quanta is lost, due to incomplete X-ray absorption and X-ray to light conversion as well as due to statistical fluctuations in the emitted optical

quanta. The decrease of the signal-to-noise-ratio from the input to the output of an X-ray imaging screen has been previously (Dainty and Shaw, 1974; Swank, 1974; Dick and Motz, 1981; Tapiovara and Wagner, 1985; Drangova and Rowlands, 1986; Ginzburg and Dick, 1993; Cavouras et al., 1996; Cavouras et al., 1997; Kandarakis et al., 1997a) theoretically or experimentally examined by evaluating the zero frequency detective quantum efficiency [DQE(0)]. The latter has been determined by means of the zero, first and second statistical moments of the emitted optical pulse height distribution, which requires demanding experimental arrangements (Dick and Motz, 1981, Drangova and Rowlands, 1986).

In the present study, a new method is proposed for determining SNR based on the experimental assessment of the X-ray luminescence efficiency (XLE) and on light emission spectrum measurements, which are well established (Ludwig, 1971) and routinely performed in our laboratory (Kandarakis et al., 1996). The signal-to-noise-ratio was evaluated as a function of screen coating weight and X-ray tube voltage for three scintillating materials ($\text{Gd}_2\text{O}_2\text{S:Tb}$, $\text{La}_2\text{O}_2\text{S:Tb}$

* Corresponding author. Present address: 37–39 Esperidon Street, Kallithea 17671, Athens, Greece. Tel.: +30-1-9594-558 (home); fax: +30-1-9594-558 (home), +30-1-5910-975 (work); e-mail: cavouras@hol.gr; cavouras@medisp.teiath.gr.

and $Y_2O_2S:Tb$) often used in radiography and in digital medical imaging systems (Arnold, 1979, Yaffe and Rowlands, 1997).

2. Material and methods

2.1. Theory

The output signal produced by an X-ray screen is represented by the mean number \bar{N}_L of optical quanta emitted by the whole screen during the measurement time interval. \bar{N}_L can be expressed as follows (Shaw and Van Metter, 1984; Bunch et al., 1987):

$$\bar{N}_L = \bar{N}_X \bar{\eta}_Q \bar{m}, \quad (1)$$

where, \bar{N}_X is the mean number of X-rays incident on the whole screen during the measuring time interval, $\bar{\eta}_Q$ is the mean X-ray quantum detection efficiency, averaged over the screen area, giving the fraction of detected X-rays, \bar{m} is the mean number of emitted optical quanta per X-ray absorbed, averaged over the screen area. \bar{m} , however, may be expressed in terms of 1/the mean number (m_0) of the optical photons generated within the screen material by an X-ray quantum and 2/the mean light transmission efficiency G_L , giving the fraction of m_0 that is transmitted to the screen emitting surface, as follows:

$$\bar{m} = \bar{m}_0 \bar{G}_L, \quad (2)$$

where \bar{m}_0 , \bar{G}_L are mean values averaged over the area of the screen.

This is equivalent to

$$\bar{m} = \overline{\eta_C \{\bar{E}/\bar{E}_\lambda\}} \bar{G}_L = \bar{\eta}_C \{\bar{E}/\bar{E}_\lambda\} \bar{G}_L, \quad (3)$$

where, $\bar{\eta}_C$ is the mean intrinsic X-ray to light conversion efficiency of a scintillator, expressing the fraction of X-ray energy transformed into light in the interior of the screen material (Ludwig, 1971) averaged over the screen area and \bar{E} , \bar{E}_λ are the mean X-ray and optical photon energies respectively. Thus, from Eqs. (1)–(3) the mean number of totally emitted quanta \bar{N}_L may be written as

$$\bar{N}_L = \bar{N}_X \bar{\eta}_Q \bar{\eta}_C \{\bar{E}/\bar{E}_\lambda\} \bar{G}_L. \quad (4)$$

The signal-to-noise-ratio is the inverse square root of the relative variance of N_L . The latter is given by the ratio of the variance over the mean value of N_L squared. The relative variance of N_L was determined by calculating and adding the relative variances of N_X , η_Q , $\eta_C \{\bar{E}/\bar{E}_\lambda\}$ and G_L . Poisson statistics were considered for X-ray photons N_X , optical quanta m_0 , and a binomial distribution probability for the efficiencies of X-ray detection η_Q and light transmission G_L (Shaw

and Van Metter, 1984). The variances considered were those corresponding to multiple events. Thus, the variance of one single event was divided by the number of events.

The relative variance in N_X , η_Q , $\eta_C \{\bar{E}/\bar{E}_\lambda\}$ and G_L corresponding to a single event may be expressed by

$$\begin{aligned} \text{var}_R(N_X) &= \frac{\text{var}(N_X)}{\bar{N}_X^2} = \frac{1}{\bar{N}_X} \\ \text{var}_R(\eta_Q) &= \frac{\bar{\eta}_Q(1 - \bar{\eta}_Q)}{\bar{\eta}_Q^2} \\ \text{var}_R(\eta_C \{\bar{E}/\bar{E}_\lambda\}) &= \frac{\text{var}(\eta_C \{\bar{E}/\bar{E}_\lambda\})}{(\bar{\eta}_C \{\bar{E}/\bar{E}_\lambda\})^2} \\ \text{var}_R(G_L) &= \frac{\bar{G}_L(1 - \bar{G}_L)}{\bar{G}_L^2}. \end{aligned} \quad (5)$$

For multiple events the number of X-ray detection, X-ray to light conversion and optical photon transmission events should be equal to \bar{N}_X , $\bar{N}_X \bar{\eta}_Q$ and $\bar{N}_X \bar{\eta}_Q \bar{\eta}_C \{\bar{E}/\bar{E}_\lambda\}$ respectively. Hence, the corresponding relative variances may be calculated as

$$\begin{aligned} \text{var}_R(\eta_Q)_M &= \frac{1}{\bar{N}_X} \left[\frac{1}{\bar{\eta}_Q} - 1 \right] \\ \text{var}_R(\eta_C \{\bar{E}/\bar{E}_\lambda\})_M &= \frac{1}{\bar{N}_X \bar{\eta}_Q} \times \frac{1}{\bar{\eta}_C \{\bar{E}/\bar{E}_\lambda\}} \\ \text{var}_R(G_L)_M &= \frac{1}{\bar{N}_X \bar{\eta}_Q \bar{\eta}_C \{\bar{E}/\bar{E}_\lambda\}} \left[\frac{1}{\bar{G}_L} - 1 \right], \end{aligned} \quad (6)$$

where subscript M in Eq. (6) denotes variance corresponding to multiple events. Thus, the relative variance in N_L may be expressed as

$$\text{var}_R(N_L) = \frac{1}{\bar{N}_X \bar{\eta}_Q} \left[1 + \frac{1}{(\bar{\eta}_C \{\bar{E}/\bar{E}_\lambda\} \bar{G}_L)} \right]. \quad (7)$$

The signal to noise ratio is given by the inverse square root of the relative variance as follows:

$$\text{SNR} = [\text{var}_R(N_L)]^{-1/2} = \left[\frac{\bar{N}_X \bar{\eta}_Q \bar{\eta}_C \{\bar{E}/\bar{E}_\lambda\} \bar{G}_L}{\bar{\eta}_C \{\bar{E}/\bar{E}_\lambda\} \bar{G}_L + 1} \right]^{1/2}. \quad (8)$$

However, the product $\bar{\eta}_Q \bar{\eta}_C \bar{G}_L$ in the numerator of the relation in Eq. (8) expresses the emitted light energy fluence (Ψ_L) over the incident X-ray energy fluence (Ψ_X) which is equivalent to the luminescence efficiency (η_Φ) (Ludwig, 1971)

$$\eta_\Phi = \frac{\Psi_L}{\Psi_X} = \eta_Q \eta_C G_L. \quad (9)$$

In this way, the signal-to-noise-ratio may be directly expressed in terms of the luminescence efficiency of the

scintillator, which can be determined experimentally

$$\text{SNR} = \left[\frac{\bar{N}_X \bar{\eta}_\Phi \{\bar{E}/\bar{E}_\lambda\}}{\bar{\eta}_C \{\bar{E}/\bar{E}_\lambda\} \bar{G}_L + 1} \right]^{1/2}. \quad (10)$$

2.2. Experimental procedure

Employing the relation in Eq. (10), SNR was determined as follows:

1. \bar{N}_X was found by performing exposure measurements and multiplying them by the appropriate conversion factor (Motz and Danos, 1978, Hendee, 1970) in order to convert exposure into X-ray fluence $\alpha(E) = \Psi/X$. To obtain the total number of X-ray quanta incident on the screen, the X-ray fluence was multiplied by the screen area, which was approximately 5 cm^2 .
2. η_Φ was determined by X-ray luminescence measurements using an EMI 9558 QB photomultiplier to measure the light energy fluence emitted by each screen. The incident X-ray energy fluence was determined from exposure measurements using the appropriate conversion factor (Hendee, 1970). Light measurements were corrected by dividing by
 1. The geometric light collection efficiency of the screen-photocathode combination giving the fraction of emitted light energy fluence which is incident on the photocathode. This geometric efficiency depends on the screen-photocathode distance and on the active areas of the screen and the photocathode. It also depends on the angular distribution of the emitted light which was measured using a photomultiplier rotating on an 180° semicircle, vertically directed with respect to the screen surface (Giakoumakis and Miliotis, 1985).
 2. The spectral matching factor (Giakoumakis, 1991) expressing the spectral compatibility between the scintillator emission spectrum, measured in our laboratory, and the spectral sensitivity distribution of the extended S-20 photocathode, obtained from manufacturer's data. N_X and η_Φ were repeatedly measured (four times) and were averaged to minimize statistical errors.
 3. \bar{E}_λ was determined from the screen emission spectrum using the relation in Eq. (11)

$$\bar{E}_\lambda = \frac{hc}{\bar{\lambda}} = hc \left[\frac{\int_{\lambda_1}^{\lambda_2} S_P(\lambda) \lambda \, d\lambda}{\int_{\lambda_1}^{\lambda_2} S_P(\lambda) \, d\lambda} \right]^{-1}, \quad (11)$$

where $S_P(\lambda)$ is the emission spectrum measured by an Oriel 7240 monochromator. $\bar{\lambda}$ is the mean light wavelength, h is Plank's constant and c is the velocity of light.

The product $\eta_C \bar{G}_L$ in Eq. (10) is defined as the X-ray to emitted light conversion efficiency (M_L) and can be determined using the relation in Eq. (9) and the measured values of the luminescence efficiency

$$\bar{M}_L = \bar{\eta}_C \bar{G}_L = \bar{\eta}_\Phi / \bar{\eta}_Q, \quad (12)$$

where, η_Q was calculated by means of Eq. (13)

$$\bar{\eta}_Q = \int_0^{E_0} S_X(E) [1 - \exp(-\mu(E)t)] dE \Big/ \int_0^{E_0} S_X(E) dE \quad (13)$$

where $\mu(E)$ is the X-ray attenuation coefficient calculated for the scintillators employed in this study from data on coefficients for the chemical elements tabulated by Storm and Israel (1967). S_X is the spectrum of X-rays calculated as described previously (Tucker et al., 1991; Cavouras et al., 1996). E_0 is the maximum X-ray energy determined by the X-ray tube voltage and t is the screen thickness (or coating weight).

Errors in our results were mainly due to systematic and statistical errors in emitted light energy fluence determination. Smaller errors may also be attributed to exposure and $S_P(\lambda)$ measurements and to η_Q and S_X calculations. The total error was estimated to be within 5%.

SNR values were determined for X-ray screens prepared in our laboratory from $\text{Gd}_2\text{O}_2\text{S:Tb}$, $\text{La}_2\text{O}_2\text{S:Tb}$ and $\text{Y}_2\text{O}_2\text{S:Tb}$ phosphor materials with various coating weight from 20 to 140 mg/cm^2 and at 70, 90 and 120 kVp X-ray tube voltages. These three materials have the same activator (Tb^{3+}) that affects emission spectra, intrinsic conversion efficiency, and decay time, but they differ in their effective atomic numbers, density and energy of the K-absorption edge. Values for these parameters are given in the Table 1. The scintillators were provided in powder form (Derby Luminescents) and the screens were prepared by sedimentation techniques on fused silica substrates (Kandarakis et al., 1997b). This technique produces screens of granular form (e.g. luminescent grains within Na_2SiO_3 binding material) like those commonly used in various X-ray imaging modalities. X-ray exposures were performed on a Siemens Stabilipan X-ray unit.

3. Results and discussion

The X-ray luminescence efficiency of $\text{Gd}_2\text{O}_2\text{S:Tb}$, $\text{La}_2\text{O}_2\text{S:Tb}$ and $\text{Y}_2\text{O}_2\text{S:Tb}$ scintillators, measured at 70, 90 and 120 kVp for various screens of coating weights from 20 to 140 mg/cm^2 , is shown in Figs. 1, 2 and 3. The corresponding numbers of X-ray quanta were 3.014×10^6 , 9.261×10^6 and 27.525×10^6 . The XLE of $\text{Gd}_2\text{O}_2\text{S:Tb}$ was found higher than that of $\text{La}_2\text{O}_2\text{S:Tb}$ or $\text{Y}_2\text{O}_2\text{S:Tb}$ in most cases. Most curves

Table 1
Values of intrinsic physical parameters of the three scintillators used

	Gd	La	Y
Atomic numbers (Z)	64	57	39
K-absorption edge (keV)	50.2	38.9	17
	Gd ₂ O ₂ S:Tb	La ₂ O ₂ S:Tb	Y ₂ O ₂ S:Tb
Densities (g/cm ³)	7.34	5.54	5.1
Intrinsic X-ray to light conversion efficiency (η_C)	0.20	0.18	0.18
Decay time (μ s)	400	400	500
Peak emission wavelengths (nm)	545	545	380, 415, 435, 545

exhibit a maximum region, the location of which varies with scintillator material and X-ray tube voltage. The ascending part of each curve is mainly caused by the X-ray absorption properties (η_Q) of the screens; η_Q increases with coating weight attaining a saturation level at relatively thick screens. Regarding the descending part in most curves it is mainly due to the light transmission properties (G_L in the relation in Eq. (9)) governed by the light attenuation effects within the scintillator. Such effects get gradually more pronounced with increasing screen coating weight. This causes a reduction of light transmission resulting in lower number of escaping optical quanta per X-ray quantum absorbed. The peak XLE of Gd₂O₂S:Tb appeared at lower screen coating weight than the other two scintillators. This may be explained by the fact that for materials of high effective atomic number and

high density, such as Gd₂O₂S:Tb, the incident X-ray quanta are rapidly absorbed at relatively low depths within the screen material. The light quanta are then mainly generated close to the irradiated scintillator surface and, hence the maximum X-ray absorption and luminescence efficiency is reached for relatively thin screens. For heavier screen coatings a large fraction of light photons is lost, since they have to penetrate longer distances within a dense material in order to escape from the screen's emitting surface.

As it can be observed from Figs. 1–3, the Gd₂O₂S:Tb XLE is continuously increasing with tube voltage while the XLE of Y₂O₂S:Tb is decreasing between 70 and 120 kVp. These differences among the three materials are due to variations in atomic number, density and K-absorption edge; the low density, low atomic number, low K-edge Y₂O₂S:Tb scintillator can

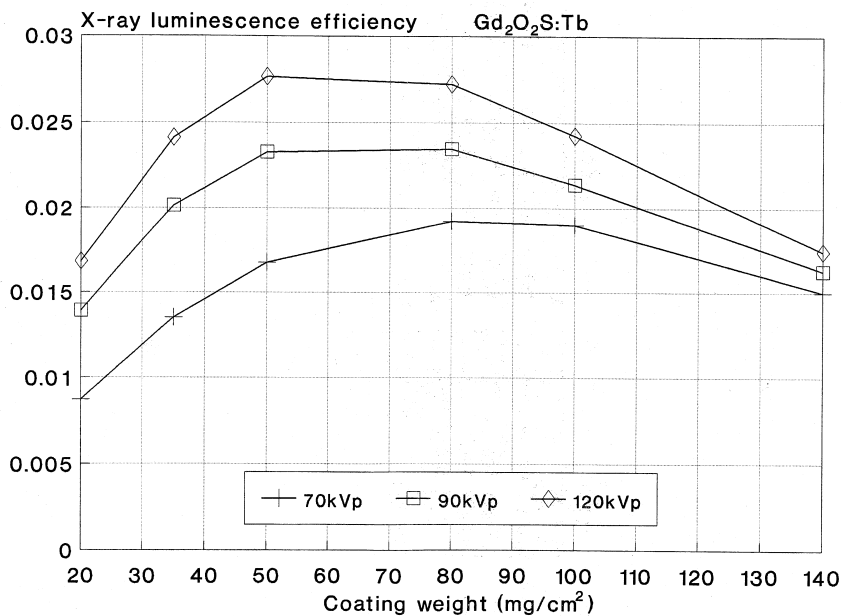


Fig. 1. X-ray luminescence efficiency of Gd₂O₂S:Tb scintillator screens.

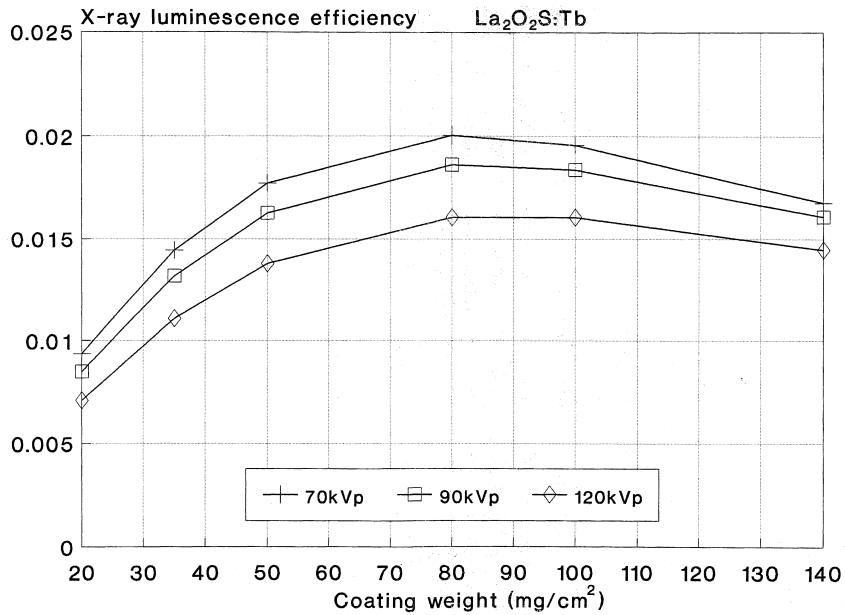


Fig. 2. X-ray luminescence efficiency of La₂O₂S:Tb scintillator screens.

not efficiently absorb X-ray quanta with energies arising from the tube voltages used in our measurements. The higher the X-ray energy the lower the absorption and, hence, the number of light photons emitted from the screen. However, in thick Y₂O₂S:Tb screens the absorption is augmented giving relatively high XLE values. The 140 mg/cm² Y₂O₂S:Tb screen emits approximately the same quantity of light as the 100 mg/

cm², whereas the 140 mg/cm² Gd₂O₂S:Tb screen (Fig. 1) exhibits 20–25% lower values than the 50–80 mg/cm² screens. In the Y₂O₂S:Tb case the light attenuation effects are overbalanced by the increased absorption while in the Gd₂O₂S:Tb case these effects reduce the intensity of the emitted light.

Figs. 4, 5 and 6 show the variation of the X-ray to emitted light conversion efficiency ($M_L = \eta_C G_L$) with

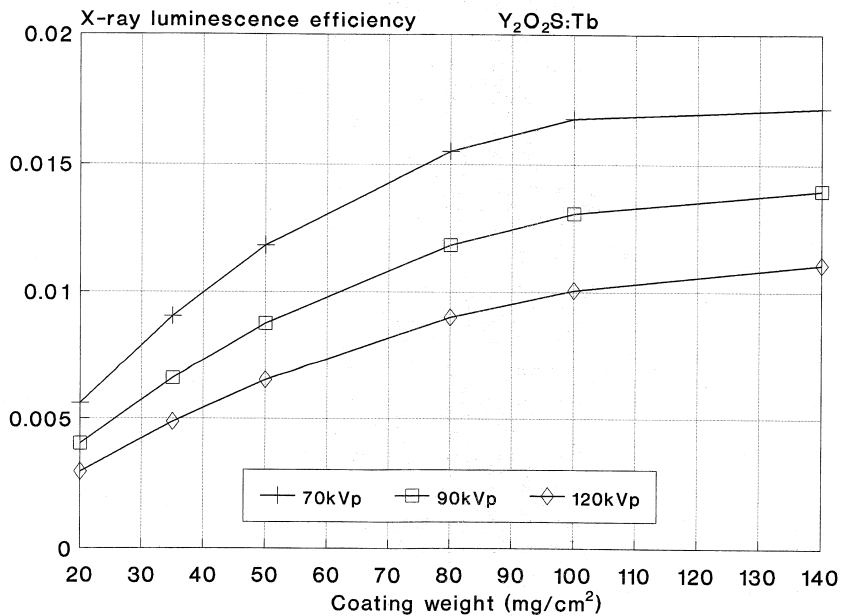


Fig. 3. X-ray luminescence efficiency of Y₂O₂S:Tb scintillator screens.

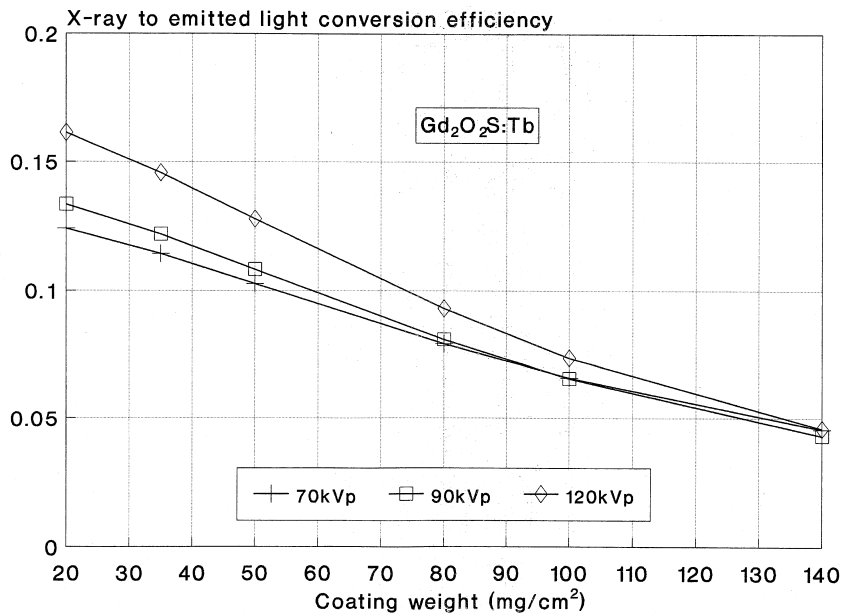


Fig. 4. X-ray to emitted light efficiency of Gd₂O₂S:Tb scintillator screens.

screen coating weight. In all cases the light generated in the interior of the scintillator (η_C) is significantly attenuated while being transmitted (G_L) through the granular structure of the screen material. This gives reduced M_L values with increasing coating. M_L depends on various parameters such as the type of ion activator (i.e. Tb³⁺), the fundamental electronic band gap of the material, the crystal structure, the size of

the luminescent grains, the light wavelength as well as the distances traveled by optical quanta to escape the screen. These distances depend on the depth of X-ray penetration prior to absorption. In the case of Gd₂O₂S:Tb, in which X-rays are mostly absorbed not deep from the exposed surface, light attenuation is more evident especially for thick Gd₂O₂S:Tb screens, due to longer average distances left for light trans-

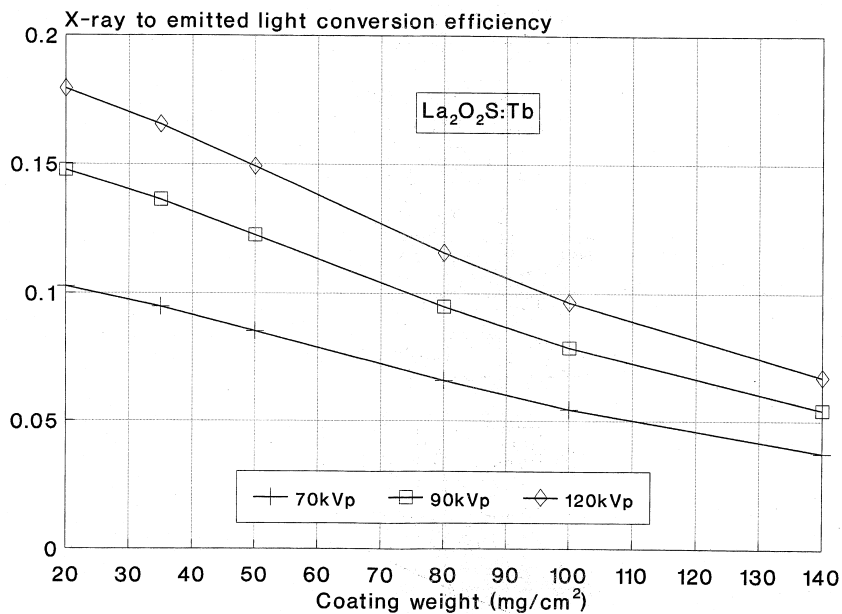


Fig. 5. X-ray to emitted light efficiency of La₂O₂S:Tb scintillator screens.

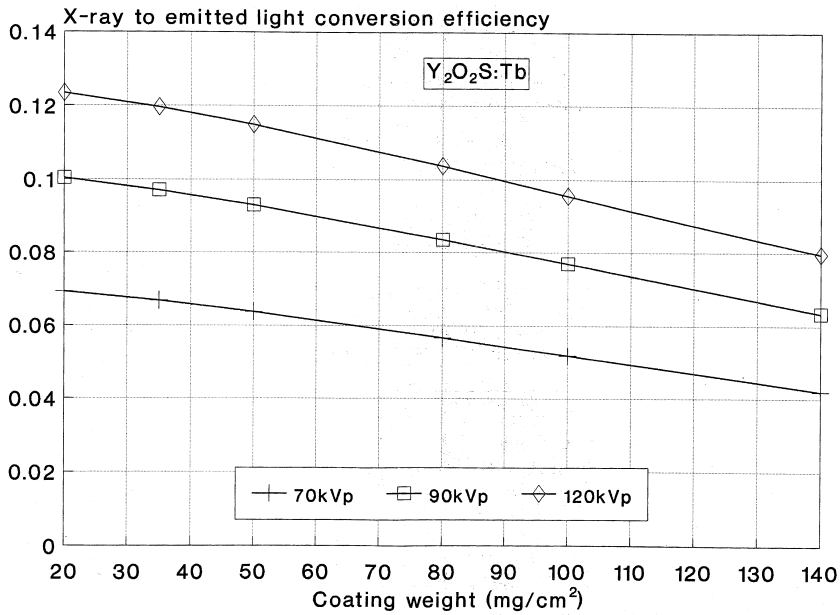


Fig. 6. X-ray to emitted light efficiency of Y₂O₂S:Tb scintillator screens.

mission to the screen output. Thus, the M_L of Gd₂O₂S:Tb is more rapidly decreasing with coating weight than the M_L of Y₂O₂S:Tb. This can be seen by comparing Figs. 4 and 6. It must be emphasized that the differences in M_L among the three materials are principally caused by variations in light transmission efficiency (G_L) rather than by different X-ray to light intrinsic conversion efficiencies (η_C). The latter has

been previously found (Kandarakis et al., 1996) approximately equal for the three materials (Table 1). It is interesting to notice that the M_L values of La₂O₂S:Tb screens, span over a wider range than in Gd₂O₂S:Tb; the M_L of La₂O₂S:Tb at 20 mg/cm², — 120 kVp was found higher than that of Gd₂O₂S:Tb, while the inverse holds at 20 mg/cm² — 70 kVp. This is because the 70 kVp X-rays correspond to an average

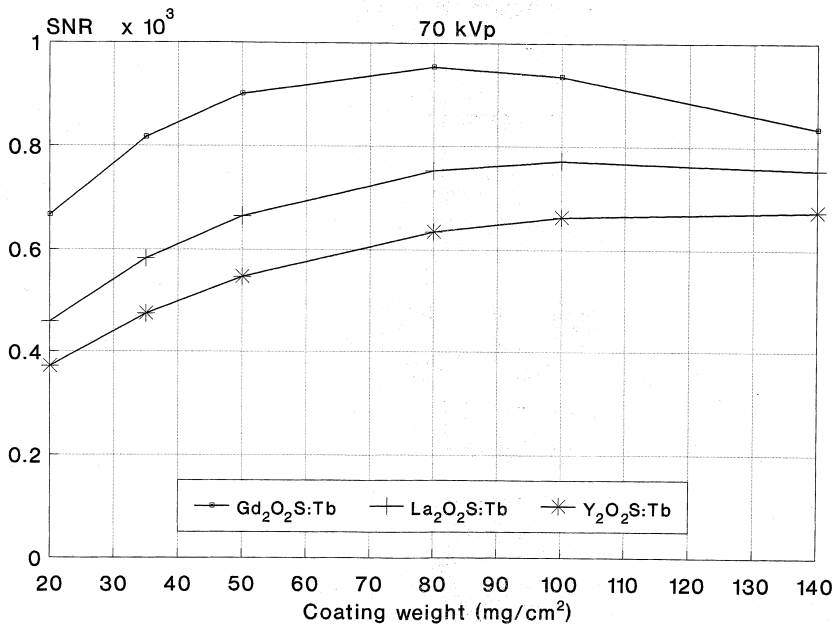


Fig. 7. Signal-to-noise-ratio of Gd₂O₂S:Tb, La₂O₂S:Tb and Y₂O₂S:Tb scintillator screens at 70 kVp X-ray tube voltage.

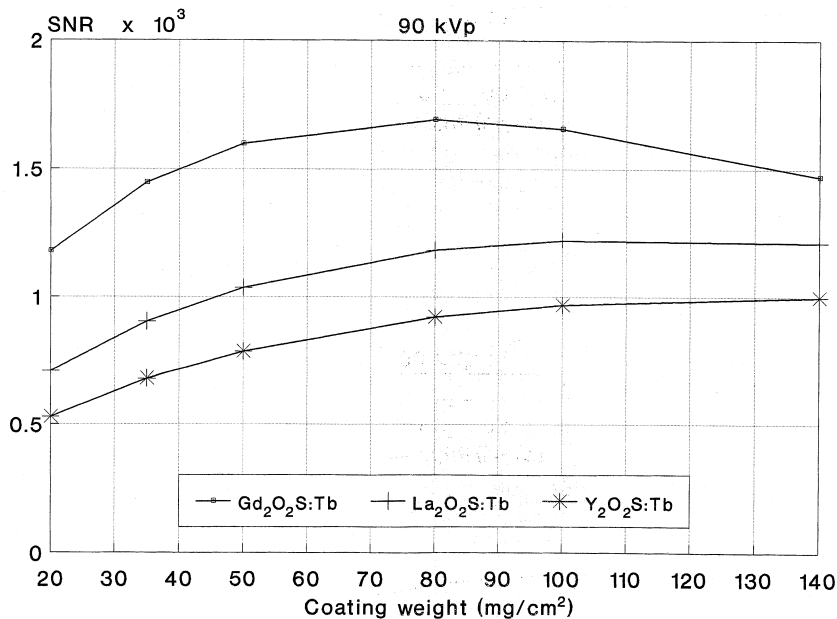


Fig. 8. Signal-to-noise-ratio of Gd₂O₂S:Tb, La₂O₂S:Tb and Y₂O₂S:Tb scintillator screens at 90 kVp X-ray tube voltage.

energy of about 45 keV which is very close to the K-absorption edge of lanthanum at 39 keV. Thus, La₂O₂S:Tb does not allow for deep X-ray penetration at 70 kVp resulting in relatively low M_L values. This property disappears gradually with increasing average X-ray energy, because the latter drifts apart from the K-edge of lanthanum. It is also of value to notice, that

the Y₂O₂S:Tb screens attain better M_L values than Gd₂O₂S:Tb and La₂O₂S:Tb at thick screens, due to deeper X-ray penetration than in the two other materials.

Figs. 7, 8 and 9 show the results obtained for the signal-to-noise-ratio of the three scintillators at 70, 90 and 120 kVp. The SNR of Gd₂O₂S:Tb was higher in

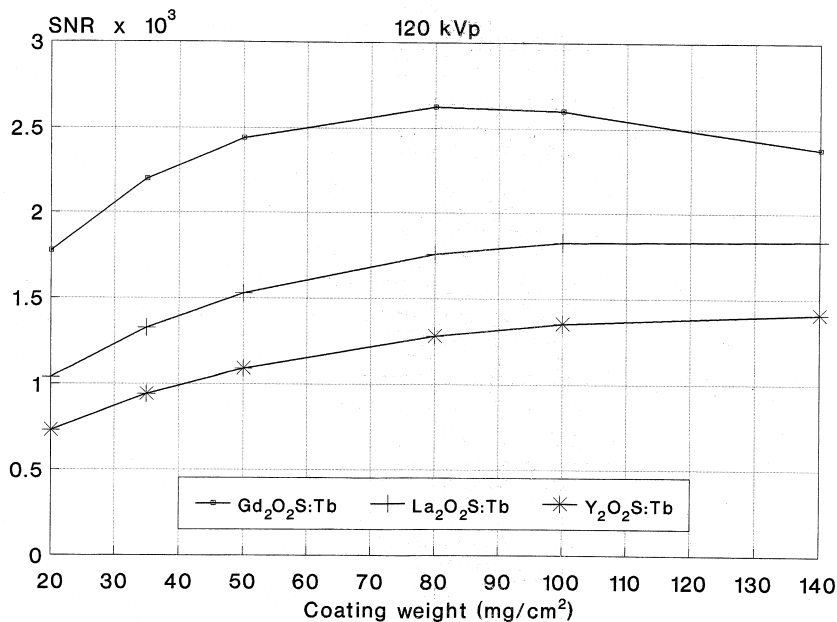


Fig. 9. Signal-to-noise-ratio of Gd₂O₂S:Tb, La₂O₂S:Tb and Y₂O₂S:Tb scintillator screens at 120 kVp X-ray tube voltage.

most tube voltage-coating weight combinations. Best results for $\text{Gd}_2\text{O}_2\text{S:Tb}$ were obtained for screens between 80 and 100 mg/cm^2 and for all X-ray tube voltages employed in our measurements (Figs. 7–9). SNR peak values are determined by the combined effect of the X-ray luminescence efficiency, which attains a peak value and decreases thereafter and the X-ray to emitted light efficiency M_L . The latter decreases with coating weight but, being in the denominator of the relation in Eq. (10) as $\eta_C G_L$, induces an inverse effect on SNR values. The X-ray to light energy ratio (\bar{E}/\bar{E}_λ) remains constant for all screens prepared from the same material. SNR differences among the three materials augment with increasing X-ray energy (Figs. 7–9) mainly due to the effect of the X-ray luminescence efficiency. The latter increases with tube voltage, in the case of $\text{Gd}_2\text{O}_2\text{S:Tb}$ screens, whereas for $\text{La}_2\text{O}_2\text{S:Tb}$ and $\text{Y}_2\text{O}_2\text{S:Tb}$ it was found decreased at high voltages (Figs. 1–3).

4. Summary and conclusions

Signal-to-noise-ratios were studied for various screens prepared from $\text{Gd}_2\text{O}_2\text{S:Tb}$, $\text{La}_2\text{O}_2\text{S:Tb}$ and $\text{Y}_2\text{O}_2\text{S:Tb}$ scintillator materials. Measurements were performed using 70, 90 and 120 kVp X-ray tube voltages, often employed in medical X-ray imaging. The method of SNR evaluation was based on the determination of the X-ray luminescence efficiency, the X-ray to emitted light conversion efficiency and the X-ray energy to light energy ratio (\bar{E}/\bar{E}_λ). All these parameters depend on the intrinsic physical properties of the scintillator materials and allow for material comparison to be employed in various imaging applications. $\text{Gd}_2\text{O}_2\text{S:Tb}$ exhibiting the highest density, effective atomic number and K-edge energy, gave best results in most cases followed by $\text{La}_2\text{O}_2\text{S:Tb}$.

Acknowledgements

This study is dedicated to the memory of Professor G.E. Giakoumakis, leading member of our team, whose work on phosphor materials has inspired us to continue.

References

Arnold, B.A., 1979. Physical characteristics of screen-film combinations In: Haus, A.G. (Ed.), *The Physics of Medical Imaging: Recording System, Measurements and*

- Techniques*. American Association of Physicists in Medicine, New York, pp. 30–71.
- Bunch, P.C., Huff, K.E., Van Metter, R., 1987. Analysis of detective quantum efficiency of a radiographic film-screen combination. *J. Opt. Soc. Am. A* 4, 902.
- Cavouras, D., Kandarakis, I., Panayiotakis, G., Evangelou, E.K., Nomicos, C.D., 1996. An evaluation of the $\text{Y}_2\text{O}_3:\text{Eu}^{3+}$ scintillator for application in medical X-ray detectors and image receptors. *Med. Phys.* 23, 1965.
- Cavouras, D., Kandarakis, I., Panayiotakis, G.S., Kanellopoulos, M., Triantis, D. and Nomicos, C.D., 1997. An investigation of the imaging characteristics of the $\text{Y}_2\text{O}_2\text{S:Eu}$ phosphor for application in X-ray detectors of digital mammography. *Appl. Radiat. Isot.* 49, 931.
- Dainty, J.C., Shaw, R., 1974. Detective quantum efficiency, signal-to-noise-ratio, and the noise-equivalent number of quanta. In: *Image Science*. Academic Press, New York, pp. 152–188.
- Dick, C.E., Motz, J.W., 1981. Image information transfer properties of X-ray fluorescent screens. *Med. Phys.* 8, 337.
- Drangova, M., Rowlands, J.A., 1986. Optical factors affecting the detective quantum efficiency of radiographic screens. *Med. Phys.* 13, 150.
- Giakoumakis, G.E., Miliotis, D.M., 1985. Light angular distribution of fluorescent screens excited by X-rays. *Phys. Med. Biol.* 30, 21.
- Giakoumakis, G.E., 1991. Matching factors for various light source-photodetector combinations. *App. Phys. A* 52, 7.
- Ginzburg, A., Dick, C.E., 1993. Image information and transfer properties of X-ray intensifying screens in the range from 17 to 320 keV. *Med. Phys.* 20, 1013.
- Hendee, W.R., 1970. *Medical Radiation Physics*. Year Book Medical Publishers, Chicago, pp. 145–148.
- Kandarakis, I., Cavouras, D., Panayiotakis, G., Agelis, T., Nomicos, C., Giakoumakis, G., 1996. X-ray induced luminescence and spatial resolution of $\text{La}_2\text{O}_2\text{S:Tb}$ phosphor screens. *Phys. Med. Biol.* 41, 297.
- Kandarakis, I., Cavouras, D., Panayiotakis, G.S., Nomicos, C., 1997a. Evaluating X-ray detectors for radiographic applications: a comparison of ZnSCdS:Ag with $\text{Gd}_2\text{O}_2\text{S:Tb}$ and $\text{Y}_2\text{O}_2\text{S:Tb}$ screens. *Phys. Med. Biol.* 42, 1351.
- Kandarakis, I., Cavouras, D., Panayiotakis, G.S., Triantis, D., Nomicos, C.D., 1997. An experimental method for the determination of spatial frequency dependent detective quantum efficiency (DQE) of scintillators used in X-ray imaging detectors. *Nucl. Instr. Meth. Phys. Res. A* 399, 335.
- Ludwig, G.W., 1971. X-ray efficiency of powder phosphors. *J. Electrochem. Soc.* 118, 1152.
- Motz, J.W., Danos, M., 1978. Image information content and patient exposure. *Med. Phys.* 5, 8.
- Shaw, R., Van Metter, R., 1984. An analysis of the fundamental limitations of screen-film systems for X-ray detection. *Proc. SPIE* 454, 128.
- Storm, E., Israel, H., 1967. Photon cross-sections from 0.001 to 100 MeV for elements 1 through 100, report LA-3753. Los Alamos Scientific Laboratory of the University of California.

- Swank, R., 1974. Absorption and noise in X-ray phosphors. *J. Appl. Phys.* 45, 4109.
- Tapiovara, M.J., Wagner, R.F., 1985. SNR and DQE analysis of broad spectrum X-ray imaging. *Phys. Med. Biol.* 30, 519.
- Tucker, D.M., Barnes, G.T., Chakraborty, D.B., 1991. Semi-empirical model for generating tungsten target X-ray spectra. *Med. Phys.* 18, 211.
- Yaffe, M.J., Rowlands, J.A., 1997. X-ray detectors for digital radiography. *Phys. Med. Biol.* 42, 1.